J. Electroanal. Chem., 144 (1983) 315–330
Elsevier Sequoia S.A., Lausanne – Printed in The Netherlands

A PHOTOELECTROCHEMICAL STUDY OF THE REDUCTION OF ALPHA LEAD DIOXIDE IN AQUEOUS SODIUM TETRABORATE

L.M. PETER

Department of Chemistry, The University, Southampton S09 5NH (England)

(Received 1st June 1982)

ABSTRACT

Reduction of thin electrodeposited films of α-PbO_2 in aqueous sodium tetraborate results in the nucleation and growth of highly resistive PbO. Transmission and photocurrent spectroscopy as well as impedance measurements have been used to follow the reduction process, and the optical and solid-state properties of the system have been derived. No evidence for the formation of non-stoichiometric oxides such as $Pb_{12}O_{19}$ was obtained, and the results could be explained by assuming that the only phases present throughout reduction were a defective form of tetragonal PbO and α-PbO_2.

INTRODUCTION

The electrochemistry of lead and its compounds has been the subject of perennial interest. The identification and characterisation of surface phases on electrodes demand the use of sensitive in-situ techniques to supplement the information available from electrochemical measurements, and in the case of lead, refreshing new perspectives have been opened by the application of Raman spectroscopy [1–3], reflectance [4] and photocurrent spectroscopy [5–8]. The last method promises to be particularly useful, since it requires levels of irradiation far lower than those employed in laser Raman spectroscopy and largely avoids the photochemical changes which are known to occur when lead oxide films on electrodes are illuminated with intense light [3,6,7]. Photocurrent spectroscopy has been used with success to study several electrochemical systems in which semiconducting phases are formed on metal substrates [9–12], and a photoelectrochemical investigation of the reduction of α-PbO_2 in an acid acetate buffer has already been reported elsewhere [5].

The present study deals with the reduction of thin electrodeposited films of α-PbO_2 in sodium tetraborate solutions. The solubility of the oxides of lead is negligibly small in this electrolyte, whereas in acid or strongly alkaline solutions dissolution and disproportionation occur. In H_2SO_4, it is likely that the disproportionation of an intermediate oxide phase leads to the formation of $PbSO_4$ and β-PbO_2, and the structural changes during the reduction of $PbSO_4$ are correspondingly complex.On its own, photocurrent spectroscopy possesses limited power to resolve the solid-state on electrochemical changes which occur during the reduction

0022-0728/83/0000-0000/$03.00

of PbO_2, and therefore simultaneous changes in ac admittance and optical transmission of the oxide films were studied. The three techniques are complementary, and taken together they offer a powerful approach to the in-situ characterisation of semiconducting electrode systems.

EXPERIMENTAL

Films of α-PbO_2 were grown at a current density of 2 mA cm^{-2} from a buffered lead acetate solution [5,13]. The results reported here were obtained using transparent electrodes constructed from conducting "Indalux" glass, although identical photocurrent behaviour was observed with a platinum substrate electrode. The PbO_2 films formed in this way have been characterised by interferometry [5] and ellipsometry [14], and their electrochemical behaviour shows that thin films consist entirely of the α-phase.

Photocurrent spectroscopy was performed using chopped monochromatic light of low intensity (typical incident photon fluxes were of the order of 10^{14} cm^{-2} s^{-1}). The optical arrangement, which was also used for single-beam transmission measurements, consisted of a 150 W high pressure xenon lamp and a holographic grating monochromator. Schott cut-off filters GG 400, GG 495 and RG 610 were used to eliminate stray and harmonic light from the output of the monochromator. The photocurrent was detected with a lock-in amplifier, and the intensity of the incident light was determined with a calibrated silicon photodiode. At the same time, the intensity of the light transmitted through the film and transparent substrate was monitored with a second silicon photodiode. The transmission of the bare substrate was measured separately in each experiment and was found to be very reproducible. The bare substrate electrodes gave no detectable photocurrent in the spectral range 350–750 nm at the sensitivities used to record the photocurrents due to the lead oxide deposit.

The electrochemical instrumentation consisted of a function generator, potentiostat, sine-oscillator and lock-in amplifier. An operational-amplifier integrator was used to obtain the charge during cyclic voltammetric measurements. Admittance measurements were made at a frequency of 1 kHz with the lock-in amplifier. A multiplexer unit was used to interface up to four signals to an X–Y recorder. All measurements were carried out at room temperature in 0.1 mol dm^{-3} solutions of sodium tetraborate (pH 9.2) made up from AnalaR reagent with triply distilled water and purged with OFN grade nitrogen. All potentials are referred to SCE.

RESULTS AND DICUSSION

Change in electrical and optical properties during potential cycling

Freshly plated electrodes were rinsed with distilled water and immersed in the borate solution. The electrode potential was then cycled two or three times at 5 mV s^{-1} to produce a reproducible cyclic voltammogram. Figure 1 shows an example of a

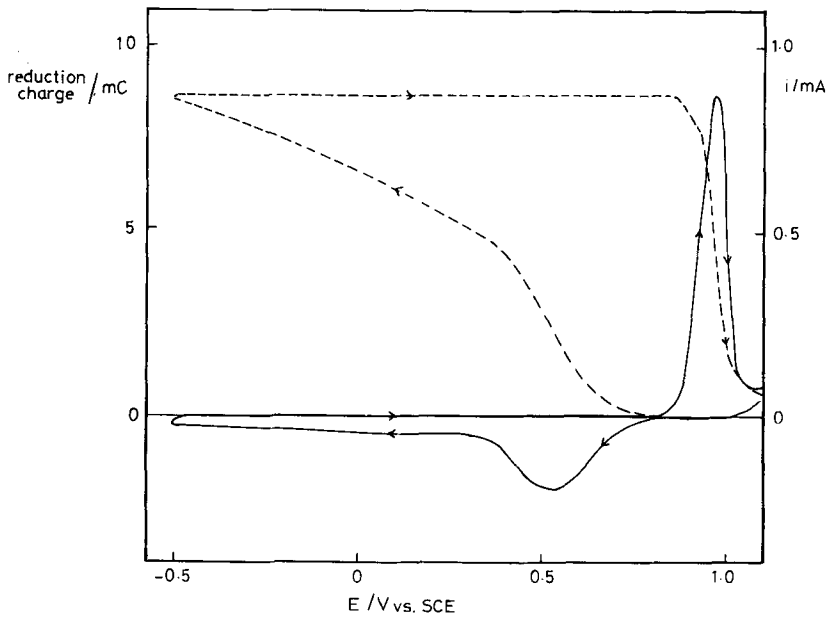

Fig. 1. Cyclic voltammogram and integrated charge (broken line) for an α-PbO_2 film in 0.1 mol dm^{-3} sodium tetraborate. Deposition charge ($Pb^{2+} \rightarrow PbO_2$) 10 mC. Sweep rate 5 mV s^{-1}. Film thickness 30 nm.

cyclic voltammogram obtained in this way. The integral of the current has also been included in the figure to demonstrate that the mean stoichiometry of the film can be cycled reversibly from PbO_2 to $PbO_{1.15}$. Irreversible changes were observed when the scan was extended to more negative values, where the nucleation of a film of lead occurred. It is clear from Fig. 1 that reduction of the α-PbO_2 film proceeds fairly readily until the mean stoichiometry of the oxide corresponds to the composition $PbO_{1.5}$. At more negative potentials, on the other hand, the current falls to a plateau, and further reduction is correspondingly slow.

The few published studies of PbO_2 reduction in alkaline media disagree significantly in their interpretation of the process. Lyamina et al. [15,16] have concluded that the reduction of α-PbO_2 in alkaline solution proceeds to $PbO_{1.39}$, whereas Chartier and Poisson [17] suggest that complete reduction to PbO takes place. Lyamina et al. have proposed that the reduction takes place without significant changes in the lattice structure, but it is not clear how this could be possible for a crystalline oxide. Although PbO_2, Pb_3O_4 and PbO are the only well-characterised thermodynamically stable oxide phases, it is known that thermal decomposition of PbO_2 gives rise to ordered metastable non-stoichiometric phases [18–21], and the results of an earlier electrochemical study by the author suggested that $Pb_{12}O_{19}$ may be formed during the reduction of α-PbO_2 [5]. Since PbO_2 and Pb_3O_4 have narrow regions of phase homogeneity, it seems likely that reduction of PbO_2 will result in

the formation of a multi-phase system. In thermal decomposition studies, the metastable phases referred to as α- and β-PbO_x are formed initially, whereas Pb_3O_4 is formed only after prolonged annealing of the sample [20,21]. Anderson and Sterns [19] have assigned the "ideal" formula $Pb_{12}O_{19}$ to Byströms β-PbO_x [18], and Angstadt et al. [20], although apparently unaware of the work of Anderson and Sterns, have confirmed that a non-stoichiometric oxide PbO_x ($1.42 < x < 1.58$) is formed by thermal decomposition of both α- and β-PbO_2. The evidence for the formation of PbO_x during thermal decomposition of PbO_2 is overwhelming, but the evidence for its formation during the electrochemical reduction of PbO_2 in sodium tetraborate is less convincing. It is true that the main reduction peak in the cyclic voltammogram corresponds to the reduction of the PbO_2 film to a *mean stoichiometry* of $PbO_{1.5}$, which lies within the range suggested for PbO_x, but it is clear that further reduction proceeds smoothly to a mean stoichiometry approaching PbO. Evidently, more information about changes in the properties of the film is needed before a sensible discussion of the reduction mechanism can be attempted.

The electronic properties of the intermediate oxides of lead have not been characterised in detail, although Pamfilov et al. [22], in a study of the conductivity and thermo emf of the lead oxides, have shown that $Pb_{12}O_{19}$ and $Pb_{12}O_{17}$ are n-type (oxygen) semiconductors, whereas Pb_3O_4 appears to be a p-type semiconductor or insulator. PbO, on the other hand, exists in orthorhombic and tetragonal modifications which exhibit amphoteric conductivity. The photoconductivity of PbO is well documented [23,24], but little is known about the photosensitivity of Pb_3O_4, $Pb_{12}O_{19}$ and $Pb_{12}O_{17}$. In an earlier report, the anodic photocurrent observed during reduction of α-PbO_2 in acid acetate solutions was attributed to an oxide of composition $Pb_{12}O_{19}$ [5]. Pavlov et al. [6,7] have discussed the photoelectrochemical behaviour of lead in H_2SO_4, and they propose that the photocurrent arises in this case from the photoactivation of the tetragonal PbO layer which is known to exist under a $PbSO_4$ membrane in this system.

Figure 2 shows the anodic photocurrent observed during reduction of α-PbO_2 in sodium tetraborate solution. It is immediately clear that the photocurrent appears only after appreciable film reduction has taken place. The photocurrent passes through a maximum when the mean film stoichiometry is close to $PbO_{1.5}$, and then falls almost to zero. The photocurrent rises on the reverse sweep, in spite of the fact that no appreciable re-oxidation current flows. As soon as re-oxidation of the film begins, the photocurrent falls rapidly once more. When the potential scan is reversed close to the photocurrent peak, a much larger response appears on the reverse sweep, although re-oxidation of the film again suppresses the photocurrent.

The thickness dependence of the photocurrent was measured for films in the range 0–0.3μm, and the peak photocurrent response was found to pass through a maximum as shown in Fig. 3. The initial increase in photocurrent with film thickness is not unexpected since the amount of light absorbed increases with thickness. The subsequent fall in photoresponse suggests that the electrical field in the reduced oxide may determine the efficiency of charge carrier separation (as the film thickness increases, the rate of bulk recombination of photoexcited carriers will increase since

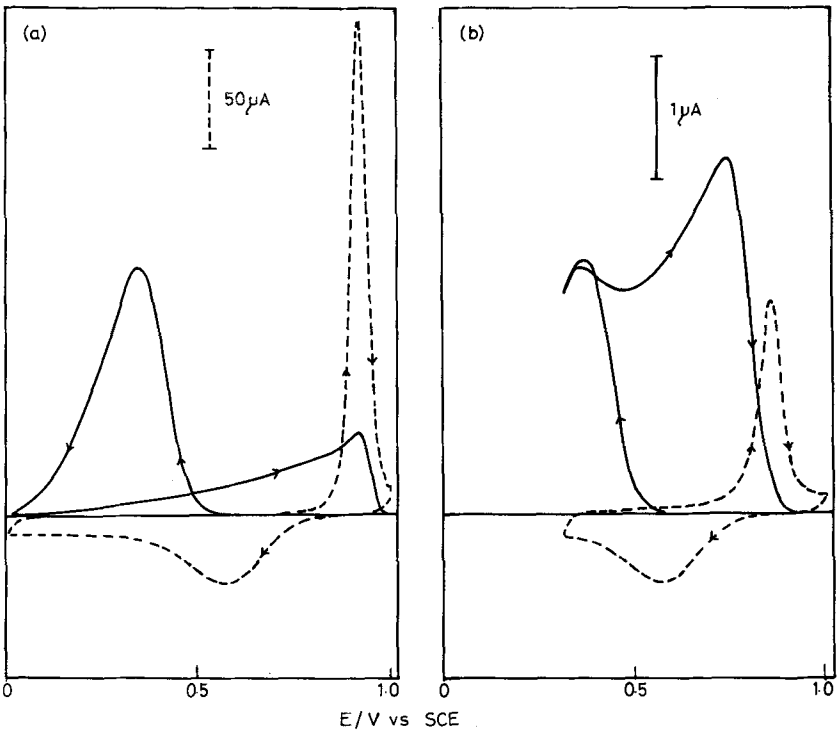

Fig. 2. Cyclic voltammograms ((— — —) and photocurrent response (———) for an α-PbO_2 film. The scales for the dark current and photocurrent are shown in (a) and (b) respectively; (b) illustrates the effect of reversing the sweep direction close to the photocurrent peak. Sweep rate 5 mV s^{-1}. Film thickness 30 nm. Excitation wavelength 400 nm.

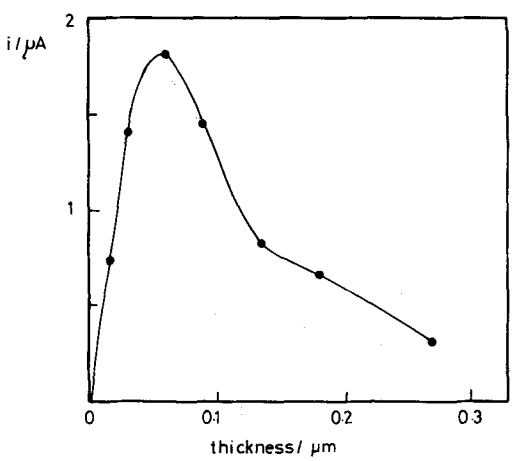

Fig. 3. Thickness dependence of maximum photocurrent during reduction at 5 mV s^{-1}. Excitation wavelength 450 nm.

the electrical field is no longer able to separate the carriers sufficiently rapidly).

The photocurrent response was measured with front and rear illumination, but no differences were observed. This important result demonstrates that reduction of the PbO_2 occurs uniformly throughout the films and excludes the possibility that the fall in photoresponse may be due to a restriction of the photoresponse to the substrate–oxide interface. The anodic photocurrent was also measured directly, and in all cases, a well-developed square response was observed.

The freshly plated PbO_2 films were a uniform brown in colour, but during reduction they became a transparent yellow. Figure 4 shows the reversible changes in transmission which occur when the electrode potential is cycled. The photocurrent excited simultaneously by the incident light is also shown in the figure, and it is clear that the onset of the photocurrent coincides with an increase in film transmission. The transmission returns to its original value when the film is reoxidised, demonstrating once again the reversibility of the system under these conditions. Since the transmission and photocurrent were measured simultaneously, it was possible to calculate the absolute quantum yield of photocurrent generation, assuming that reflection losses at the oxide/solution interface are negligible.

The rapid increase in transmission which accompanies the appearance of the photocurrent indicates that the properties of the oxide change appreciably in this part of the potential sweep. This conclusion was confirmed by simultaneous mea-

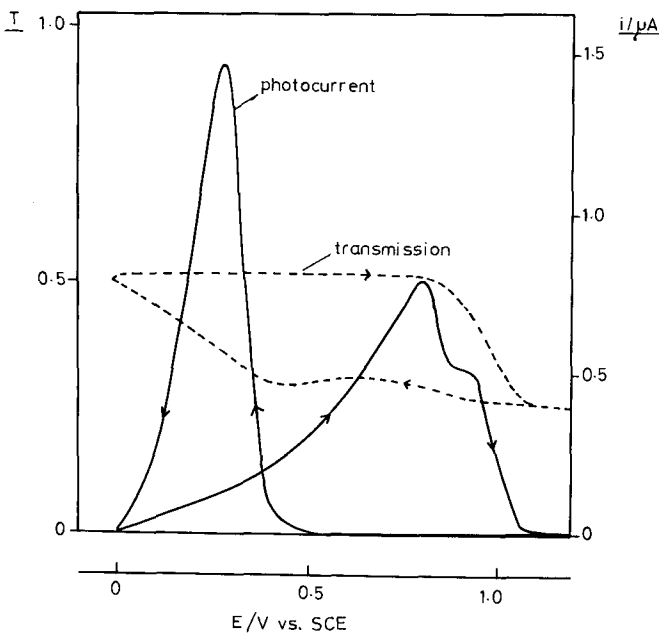

Fig. 4. Comparison of photocurrent response and optical transmission during potential cycling of α-PbO_2. Sweep rate 5 mV s^{-1}, wavelength 450 nm, film thickness 60 nm.

surement of the electrode admittance, Fig. 5. At 1.2 V vs. SCE, the positive limit of the potential scan, the in-phase component of the electrode admittance is largely determined by the solution resistance between the tip of the Luggin probe and the electrode. The resistance of the PbO_2 film itself is negligible, since the material exhibits the metallic behaviour expected for a degenerate n-type semiconductor. Evidently the film resistance remains low during the first stages of reduction. The sudden fall in admittance at 0.5 V vs. SCE provides clear proof that the conductivity of the reduced oxide decreases rapidly over a narrow range of mean film stoichiometry, and below 0.4 V vs. SCE the film appears to be an insulator.

The absence of a clear dependence of the resistance on film thickness indicates that the limiting value is probably determined by the short-circuits through small electrolyte-filled pores in the deposit, but the bulk conductivity of the reduced oxide must certainly be lower than $10^{-7}\ \Omega^{-1}$ cm. On the reverse sweep, the admittance increases again to the limiting value characteristic of the quasi-metallic α-PbO_2 film.

Analysis of absorption and photocurrent excitation spectra

A detailed series of measurements was carried out by a stepwise reduction of the electrode potential from 1.2 V vs. SCE. Integration of the current showed that the mean stoichiometry tended fairly quickly towards a constant value characteristic of the potential chosen, allowing measurement of the photocurrent and absorption spectra for films of different mean composition. The absorption coefficient was calculated directly from the film transmission (i.e. the reflectance was assumed to be negligible), and Fig. 6 shows a set of absorption spectra for films of different mean

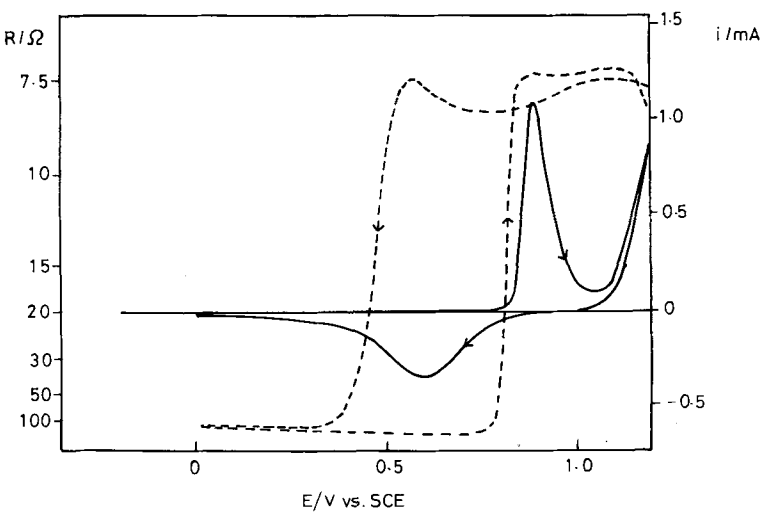

Fig. 5. Electrode admittance (— — —), measured at the same time as the cyclic voltammogram (———). Sweep rate 5 mV s^{-1}. Film thickness 270 nm.

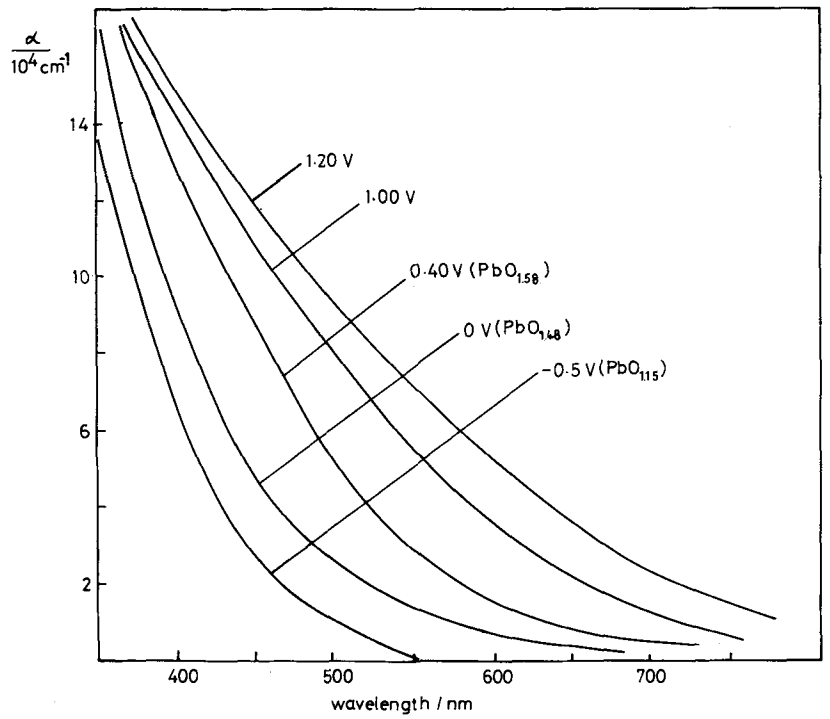

Fig. 6. Absorption spectra for an oxide film at different stages during its reduction. The mean stoichiometry of the film was calculated from the integrated reduction charge. Film thickness 150 nm.

stoichiometry (the film composition at 1.2 V and 1.0 V vs. SCE was assumed to correspond to PbO_2 since no reduction charge passes at these potentials). The spectra for the unreduced PbO_2 film are in very close agreement with the results of Mindt [25].

The analysis of the absorption spectra of semiconductors is often approached using the following general relationship [26,27]

$$\alpha h\nu = A(h\nu - E_g)^n \tag{1}$$

where $n = 1/2$ for direct allowed transition, $n = 3/2$ for indirect allowed transition and $n = 2$ for direct forbidden transition, and A is a constant. Equation (1) (with $n = 2$) has also been widely used to treat absorption spectra of amorphous semiconductors [28]. (The more exact expression in the case of forbidden transitions approximates to this general form when $(h\nu - E_g)$ is larger than the characteristic photon energy). The photocurrent excitation spectra can also be related to the absorption coefficient, provided that a simple homogeneous semiconductor phase is considered. If we assume that the electrical field extends throughout the film, the photocurrent conversion efficiency, Φ, is given by

$$\Phi = \eta\{1 - \exp(-\alpha L_f)\} \tag{2}$$

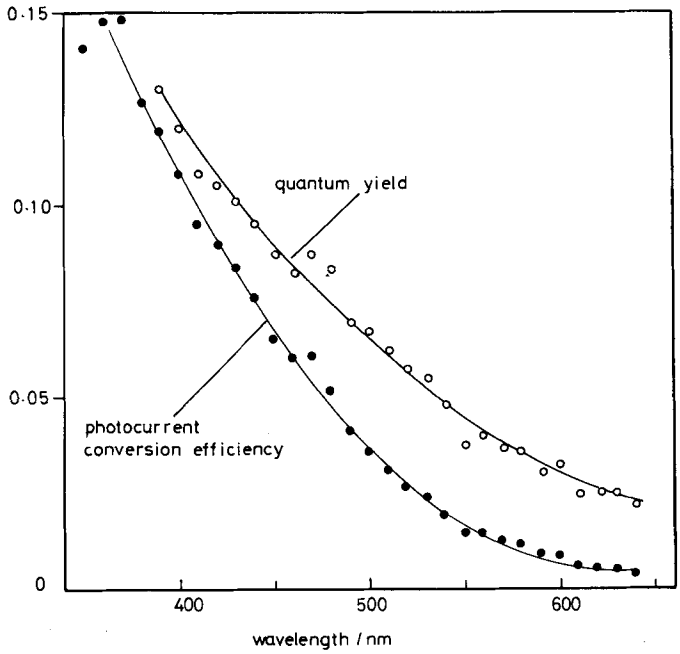

Fig. 7. Wavelength dependence of the photocurrent conversion efficiency (Φ) and quantum yield (η). Front illumination. Film thickness 150 nm.

where η is the quantum yield for photoexcited carrier collection, and L_f is the film thickness. In the cases where the Schottky length, L_s, is smaller than the film thickness, a good approximation is obtained by replacing L_f by L_s in eqn. (2). This approximation neglects the diffusion of minority carriers into the space-charge region, but this assumption is usually justifiable for polycrystalline semiconductors.

Figure 7 shows the wavelength dependence of Φ and η. The quantum yield for charge carrier collection is accessible in this case, since the amount of light absorbed in the film is known. Identical plots were obtained when the electrode was illuminated from the rear, so that the wavelength dependence of η cannot be attributed to an inhomogeneous distribution of photoactive material. The most likely explanation for the fall in η at long wavelengths is that we are not dealing with a simple homogeneous single-phase system. In a two-phase system, the absorption spectrum and photocurrent spectrum will differ if only one component is responsible for the photoeffect. For example, any PbO_2 left in the film will absorb light without contributing to the photocurrent. Further analysis of the absorption spectra reveals that a two-phase mixture must indeed be formed during reduction of α-PbO_2.

The absorption spectrum of α-PbO_2 is already potential dependent in a region where no measurable reduction has taken place (in Fig. 6, for example, the absorption spectra at 1.2 V and 1.0 V are quite different). Figure 8 shows absorption

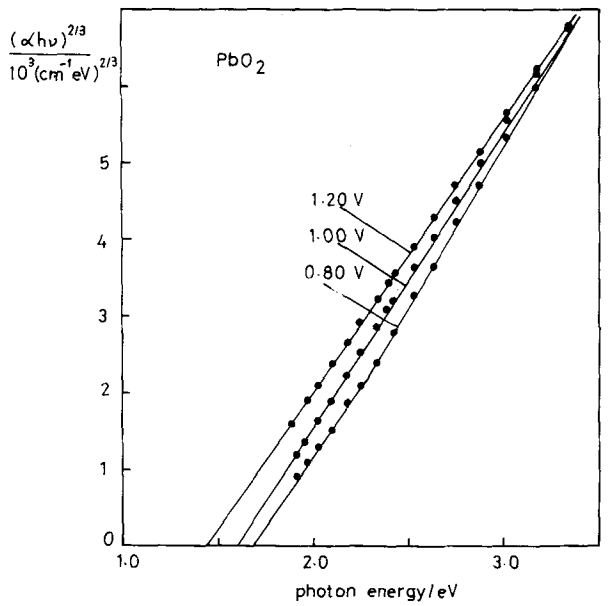

Fig. 8. Plots of absorption spectra of α-PbO_2 to test for direct forbidden transitions. The plots illustrate the shift of the absorption edge to higher photon energies which is brought about by an increase in free electron density in the oxide.

coefficient data for films at 1.2 V, 1 V and 0.8 V vs. SCE in plots appropriate for direct forbidden optical transitions. The intercept on the photon energy axis is the apparent optical band-gap, which in the case of a degenerate n-type semiconductor exceeds the true band gap since states in the conduction band are filled (i.e. the Fermi level, E_f, lies within the conduction band). The shift in photon energy is given by [25,29]

$$\Delta(h\nu) \cong \{1 + (m_e^\star/m_h^\star)\}E_f \tag{3}$$

where $m_e^\star$ and $m_h^\star$ are the effective masses of electrons and holes, and E_f for an ideal degenerate Fermi gas is related to the free electron density:

$$E_f = (3/\pi)^{2/3}(h^2/8m_e^\star)n^{2/3} \tag{4}$$

The shift in apparent band-gap which occurs when the electrode potential is changed from 1.2 V to 1.0 V vs. SCE can therefore be interpreted as evidence for an increase in free electron density in the α-PbO_2. In the absence of an independent measurement of the free-carrier density, it is not possible to calculate the true band gap of α-PbO_2, but clearly it must be lower than 1.4 eV. However, the change in free carrier density between 1.2 V and 1.0 V can be estimated from eqn. (3). If we assume $m_h^\star \gg m_e^\star$ and use Mindt's value of $m_e^\star = 0.8\ m_0$, the change in carrier density is $\Delta n \simeq 1.8 \times 10^{20}$ cm^{-3}. Mindt [25] has reported a carrier concentration of 1.4×10^{21}

cm^{-3} for α-PbO_2 measured in air, but has calculated a band-gap of 1.45 eV from a less satisfactory linear treatment of the absorption data. Lappe [30] has given a value of 1.5 eV for the band-gap, and Shapiro [31] a higher value of 1.8 eV, but the results presented here show that these values are too high. For example, if we assume a carrier density of 10^{21} cm^{-3} at 1.0 V, the band-gap will be only 1 eV.

The graphical treatment of the spectrum of 0.8 V reveals a break in slope, and in this case it seems probable that a phase-change has already begun. At potentials below 0.8 V, measurable reduction of the film takes place. Plots of absorption data appropriate for direct allowed transitions are shown in Fig. 9 for films of different mean stoichiometry. The plots show a clear break as soon as film reduction begins, and the intercepts move to higher photon energies as reduction proceeds. Experimental data for tetragonal PbO [32] have also been included for comparison. The simplest explanation for the appearance of the change in slope of the plot is that reduction results in the formation of a two-phase mixture of α-PbO_2 and a lower oxide. Although the absorption edge moves towards the curve characteristic of tetragonal PbO, it never reaches it, even when the mean film stoichiometry is $PbO_{1.15}$. An alternative explanation for the break in the plot is that indirect allowed transitions are involved in the low-energy end of the absorpion spectrum. Analysis of the photocurrent spectrum shown in Fig. 7 makes this interpretation less attractive. The fall in apparent quantum yield η with increasing wavelength is not expected

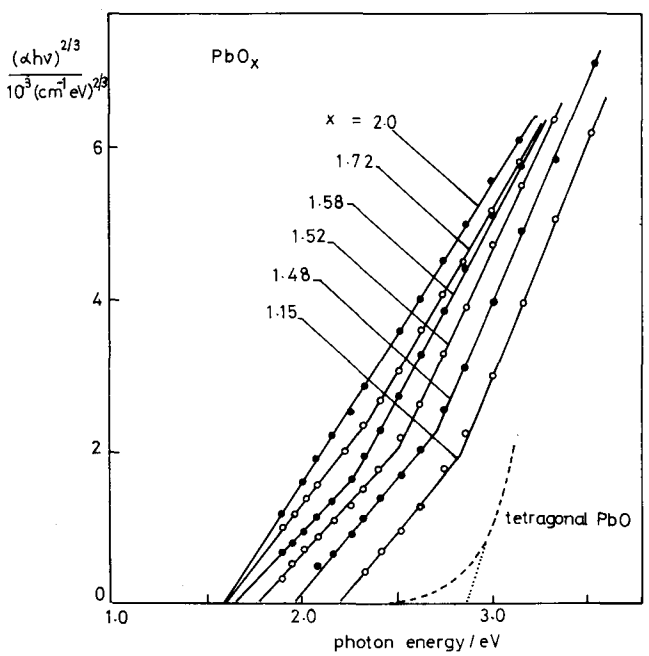

Fig. 9. Plots of absorption spectra for partially reduced films of α-PbO_2 (see Fig. 6 for original spectra). The data for tetragonal PbO were taken from ref. 32. x refers to the mean stoichiometry of the film.

for a homogeneous phase, whereas just such an effect will appear if photoinactive α-PbO_2 is left in the film during reduction, since it absorbs an appreciable fraction of the light at longer wavelengths.

If we assume that η is in fact independent of wavelength, the value of α can be estimated from eqn. (2). Figure 10 contrasts the absorption spectrum obtained in this way with published data for tetragonal [32] and orthorhombic [33] PbO (for simplicity η has been taken as unity in the calculation). The absorption spectrum derived from the photocurrent is considerably red-shifted with respect to tetragonal PbO, and shows no similarity with orthorhombic PbO. It is known that the incorporation of oxygen into PbO shifts the absorption spectrum to longer wavelengths, and the absorption spectrum of Pb_3O_4 also extends further into the red than tetragonal PbO [34,35].

A direct comparison of the measured absorption spectrum and the spectrum derived from the photocurrent is revealing. Figure 11 shows that the photocurrent spectrum can be related to a direct forbidden transition at 2.05 eV. By contrast, the upper part of the plot of the absorption data extrapolates to the same value of the

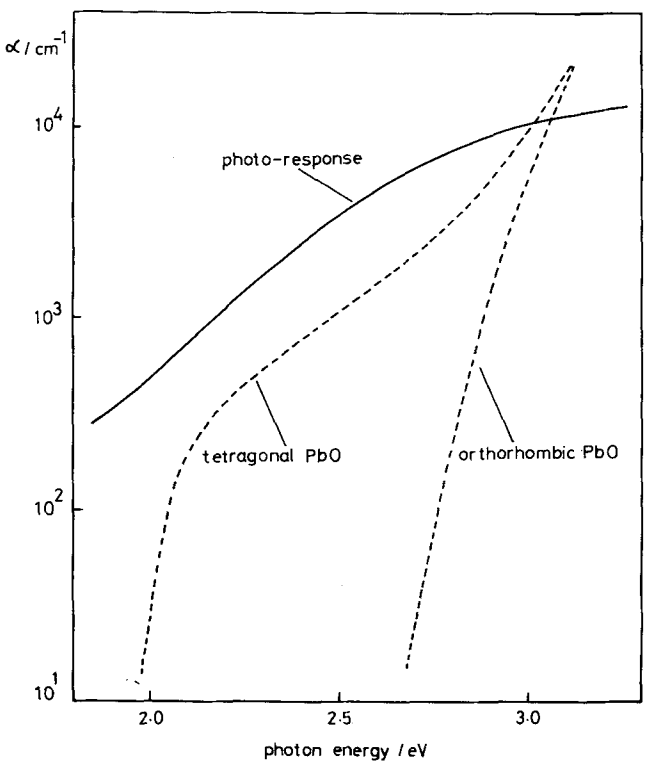

Fig. 10. Comparison of published absorption data for tetragonal [32] and orthorhombic [33] PbO with the spectrum derived from the photocurrent response of a partially reduced α-PbO_2 film.

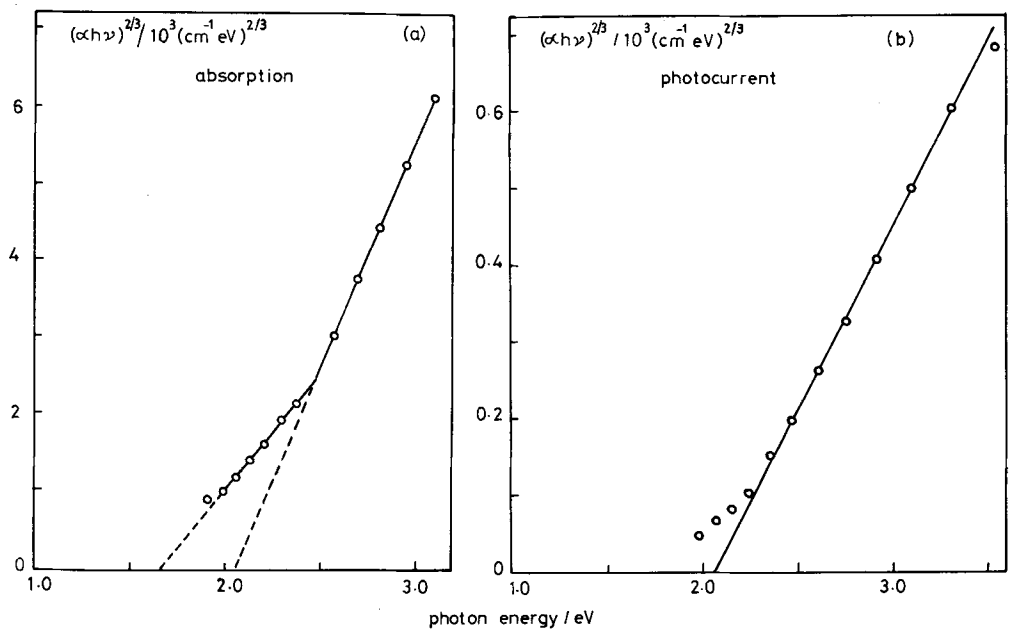

Fig. 11. Plots of absorption (a) and photocurrent (b) spectra showing direct forbidden transition at 2.05 eV. The appreciable absorption due to residual α-PbO_2 is evident in (a) as a "tail" at low photon energies.

band gap, but the absorption at lower photon energies is appreciably higher. A reasonable fit to the data in this case was obtained by assuming that the film was composed of a mixture of PbO and α-PbO_2.

The mechanism of reduction

The appearance of the photocurrent clearly coincides with a rapid increase in film resistance. The sign of the photocurrent provides proof that an electrical field is present in the oxide film which drives holes to the oxide/solution interface. This situation arises for an n-type semiconductor under depletion conditions and also for insulating materials. In the presence of oxygen, tetragonal PbO displays p-type semiconductivity, but no evidence for p-type behaviour was found with the electrochemical system (although cathodic photocurrents have been observed during the oxidation of lead in H_2SO_4 [36]). Since the oxide resistivity is high, it seems probable that an insulating phase is formed by the reduction of α-PbO_2. The low conductivity may result from the inclusion of donor impurities which bring about compensation of the p-type conductivity due to acceptor states. The red-shift in the absorption and photocurrent spectra relative to the spectrum for tetragonal PbO suggests that the oxide is disordered and may contain defect centres. High resolution electron microscopy [37] has shown that α-PbO_2 contains extensive disordered regions, and the reduction process may also lead to a phase with a similar degree of disorder.

The way in which the film resistance and photoresponse change with mean stoichiometry during reduction allows discussion of the mechanism of film reduction. Although the spectroscopic data show that the system becomes heterogeneous as soon as the electrode potential falls below 0.8 V, the mean stoichiometry falls to $PbO_{1.5}$ before the resistance increases and the photocurrent appears. In principle, the nucleation of the PbO phase could occur within the bulk of oxide by the "condensation" of oxygen vacancies in the α-PbO_2 lattice. On the other hand, the elimination of oxygen from the lattice by the reaction

$$PbO_2 + H_2O + 2\,e^- \rightarrow PbO + 2\,OH^- \qquad (5)$$

could lead to the nucleation of the PbO phase at the oxide/solution interface. This will occur as soon as the density of oxygen vacancies at the interface exceeds a critical value. Some limiting cases are illustrated in Fig. 12. If the rate of lateral expansion of PbO centres formed at the surface is rapid, a thin insulating film of PbO will form on the outside of the electrode (Fig. 12a). The experimental results do not support this model, since it predicts a smooth increase in film resistance and photoresponse as film reduction proceeds. If, on the other hand, the PbO phase grows by the three-dimensional expansion of centres which nucleate at the oxide/solution interface (Fig. 12b), the film resistivity will only change when significant overlap occurs. The mean stoichiometry of the film at this point will depend on the number density of nuclei formed, but in general the film resistance will increase rapidly over a fairly narrow range of mean stoichiometry as overlap

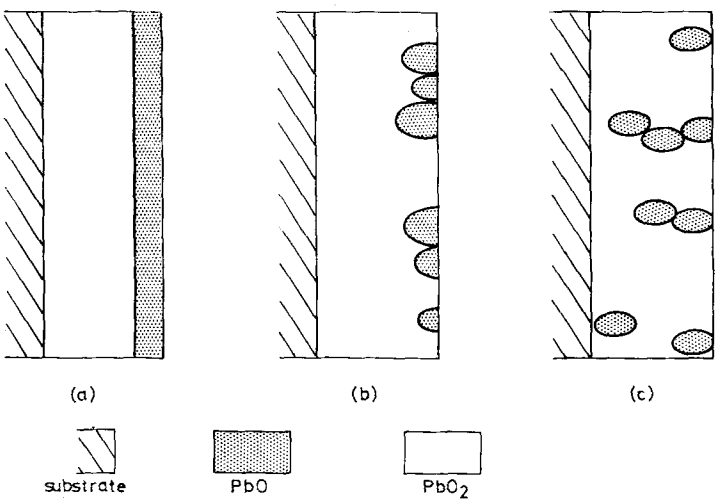

Fig. 12. Models for the nucleation and growth of PbO from the α-PbO_2 phase. In (a), a thin layer of PbO is formed before growth penetrates into the bulk. In (b), three-dimensional growth of nuclei occurs at the oxide/solution interface, leading to a more homogeneous distribution of material. In (c), PbO centres from within the bulk of the α-PbO_2. Subsequent overlap and expansion to the surfaces of the film occurs, leading to conditions under which a photoresponse can appear.

occurs. The growth process in this second model can be presumed to involve the migration of oxygen vacancies in the α-PbO_2. A third possibility is that islands of PbO form in the bulk of the α-PbO_2 deposit. Isolated centres which do not have contact to the electrolyte will be effectively "short-circuited" by the conducting α-PbO_2 matrix, and should therefore not contribute to the photocurrent. Expansion and overlap of these centres will then lead to a photocurrent as soon as contact with the electrolyte is established (Fig. 12c). The experimental results do not allow a distinction between the last two mechanisms to be made, but further support to the growth mechanism shown in Fig. 12c is provided by the observation that the photocurrent response was identical for front and rear illumination. If the growth centres expand in three dimensions, they may extend through most of the film at the point where the photocurrent response is measured. By contrast, the surface layer of PbO shown in Fig. 12a would clearly give rise to different photoexcitation spectra for front and rear illumination, and this was not observed experimentally.

The shape of the photocurrent-voltage response can now be interpreted. As reduction proceeds, PbO centres form, either at the oxide solution interface or in the bulk, and expand by conversion of the α-PbO_2. At first the film resistance is negligible, and the field is too small to separate charge carriers generated by light absorbed in the PbO. When the PbO centres begin to overlap, the film resistance rises sharply and the resulting electrical field developed across the oxide begins to separate the photoexcited carriers. The resistivity increases further as the film is converted almost entirely to PbO, although islands of PbO_2 remain trapped in the film after overlap of the expanding growth centres. On the cathodic sweep, however, the electrical field falls in spite of the increase in film resistance, since the electrode potential is moving towards the flat-band potential of the oxide. As a result the efficiency of carrier separation decreases and the photocurrent again falls towards zero. The flat-band potential of the PbO can therefore be estimated to lie at a potential negative of 0 V vs. SCE. (Hardee and Bard [38] give a value of -0.3 V vs. SCE at pH 9 for the flat-band potential of PbO formed by direct oxidation of the metal.) When the sweep is reversed, the electrical field increases once more and the photocurrent rises until the stoichiometry of the oxide begins to change as re-oxidation takes place. The field in the oxide then collapses as the PbO is converted back to PbO_2.

The experimental observations made in this study lend little support to an earlier conclusion that the photoresponse is due to a PbO_x phase such as $Pb_{12}O_{19}$ [5]. It is clear from the absorption and photocurrent spectra that reduction leads to a multiphase system, so that a simple interpretation on the basis of the mean stoichiometry is no longer permissible. Further ex-situ studies are needed to examine the phases formed during the reduction of α-PbO_2, and these are now planned. Attempts are also being made to relate the results of this study to a detailed photoelectrochemical examination of the behaviour of lead in acid and alkaline solutions [39].

ACKNOWLEDGEMENTS

The author thanks R. Peat and N.P. Freestone for discussions on this work.

REFERENCES

1 R.J. Thibeau, C.W. Brown, A.Z. Goldfarb and R.H. Heidersbach, J. Electrochem. Soc., 127 (1980) 37.
2 R.J. Thibeau, C.W. Brown, A.Z. Goldfarb and R.H. Heidersbach, J. Electrochem. Soc., 127 (1980) 1702.
3 R. Varma, C.A. Melendres and N.P. Yao, J. Electrochem. Soc., 127 (1980) 1416.
4 K.D. Naegele and W.J. Plieth, Electrochim. Acta, 25 (1980) 241.
5 L.M. Peter, Surf. Sci., 101 (1980) 162.
6 D. Pavlov, Z. Zanova and G. Papazov, J. Electrochem. Soc., 124 (1977) 1522.
7 D. Pavlov, J. Electroanal. Chem., 118 (1981) 167.
8 R.G. Barradas, D.S. Nadezhdin, J.B. Webb, A.P. Roth and D.F. Williams, J. Electroanal. Chem., 126 (1981) 273.
9 L.M. Peter, Electrochim. Acta, 23 (1978) 1073.
10 L.M. Peter, J. Electroanal. Chem., 98 (1979) 49.
11 M.I. da Silva Pereira and L.M. Peter, J. Electroanal. Chem., 131 (1982) 167.
12 J.F. McAleer and L.M. Peter, Faraday Discuss. Chem. Soc., 70 (1980) 67.
13 M. Fleischmann and M. Liler, Trans. Faraday Soc., 54 (1958) 1370.
14 R. Greef, unpublished work.
15 L.I. Lyamina, N.I. Korolkova and K.M. Gorbunova, Sov. Electrochem., 6 (1970) 389.
16 L.I. Lyamina, N.I. Korolkova, E.K. Oshe and K.M. Gorbunova, Sov. Electrochem., 10 (1974) 841.
17 P. Chartier and R. Poisson, Bull. Soc. Chim. Fr., (1969) 2255.
18 A. Byström, Ark. Kemi Mineral. Geol., 20 A (1945) 1.
19 J.S. Anderson and M. Sterns, J. Inorg. Nucl. Chem., 11 (1959) 272.
20 R.-T. Angstadt, C.J. Venuto and P. Ruetschi, J. Electrochem. Soc., 109 (1962) 177.
21 S.M.Caulder and A.C. Simon, J. Electrochem. Soc., 121 (1974) 1546.
22 A.V. Pamfilov, E.G. Ivanchevka and P.V. Drogomiretskii, Russ. J. Phys. Chem., 41 (1967) 565.
23 R.C. Keezer, D.L. Bowman and J.H. Becker, J. Appl. Phys., 39 (1968) 2062.
24 J. van den Broek, Solid Stat. Commun., 4 (1966) 295.
25 W. Mindt, J. Electrochem. Soc., 116 (1969) 1076.
26 G. Harbeke in F. Abelès (Ed.), Optical Properties of Solids, North-Holland, Amsterdam, London, 1972, p. 21.
27 J.I. Pankove, Optical Processes in Semiconductors, Prentice-Hall, Englewood Cliffs, 1971, p. 34.
28 J. Tauc in ref. 26, p. 277.
29 E. Burstein, Phys. Rev., 93 (1954) 632.
30 F. Lappe, J. Phys. Chem. Solids, 23 (1962) 1563.
31 I.P. Shapiro, Opt. Spektrosk., 4 (1958) 256.
32 J. van den Broek, Philips Res. Rep., 22 (1967) 36.
33 K. Iinuma, T. Seki and M. Wada, Mat. Res. Bull., 2 (1967), 527.
34 V.A. Izvozchikov, E.M. Shamba and S.R. Kishmariya, Zh. Prikl. Spektrosk., 20 (1974) 902.
35 V.A. Izvozchikov, Phys. Status Solidi, (a) 14 (1972) 161.
36 L.M. Peter, unpublished data.
37 P.T. Moseley, J.L. Hutchison and M.A.M. Bourke, J. Electrochem. Soc., 129 (1982) 876.
38 K.L. Hardee and A.J. Bard, J. Electrochem. Soc., 124 (1977) 215.
39 N.P. Freestone and L.M. Peter, in preparation.